

to a greater withdrawal of electron density from the metal center, a subsequent lowering in energy of the HOMO, and thus an increase in the $E_{1/2}$ values; however, differences in σ -donor abilities are also a likely contributing factor.

Reactions of $[\text{Re}_2(\mu\text{-H})_4\text{H}_3(\text{PPh}_3)_4(\text{CN-}t\text{-Bu})](\text{PF}_6)_2$ and $[\text{Re}_2(\mu\text{-H})_3\text{H}_2(\text{PPh}_3)_4(\text{CN-}t\text{-Bu})_2](\text{PF}_6)_2$ with *tert*-Butyl Isocyanide. Whereas neither of the diamagnetic congeners of these two complexes reacts with excess *tert*-butyl isocyanide over reasonable periods of time, both the paramagnetic dications react quite rapidly (Scheme I). The dirhenium heptahydrido species reacts in dichloromethane to afford a 3:1 mixture of $[\text{Re}_2(\mu\text{-H})_3\text{H}_2(\text{PPh}_3)_4(\text{CN-}t\text{-Bu})_2]\text{PF}_6$ and $[\text{Re}(\text{CN-}t\text{-Bu})_4(\text{PPh}_3)_2]\text{PF}_6$ (as monitored by CV). In this reaction H_2 was identified by GC analysis as the only volatile gaseous product. When $[\text{Re}_2(\mu\text{-H})_3\text{H}_2(\text{PPh}_3)_4(\text{CN-}t\text{-Bu})_2](\text{PF}_6)_2$ is reacted in this same fashion, the major product was the reduced monocation plus some $[\text{Re}(\text{CN-}t\text{-Bu})_4(\text{PPh}_3)_2]\text{PF}_6$ (ca. 4:1 ratio of products).²⁷ Thus the formation of the diamagnetic monocationic dirhenium polyhydride species serves as a hindrance to the rapid and complete evolution of H_2 and the formation of the thermodynamic product $[\text{Re}(\text{CN-}t\text{-Bu})_4(\text{PPh}_3)_2]\text{PF}_6$. This being the case, we reasoned that by keeping $[\text{Re}_2(\mu\text{-H})_3\text{H}_2(\text{PPh}_3)_4(\text{CN-}t\text{-Bu})_2]^{2+}$ in its oxidized state, i.e., preventing back reaction to the much more kinetically inert monocation, complete and rapid conversion to $[\text{Re}(\text{CN-}t\text{-}$

$\text{Bu})_4(\text{PPh}_3)_2]^+$ could be accomplished. This was proven by carrying out the reaction between $[\text{Re}_2(\mu\text{-H})_3\text{H}_2(\text{PPh}_3)_4(\text{CN-}t\text{-Bu})_2](\text{PF}_6)_2$ and *tert*-butyl isocyanide in a CV cell at a potential of +0.50 V; this prevented reduction back to $[\text{Re}_2(\mu\text{-H})_3\text{H}_2(\text{PPh}_3)_4(\text{CN-}t\text{-Bu})_2]^+$ while at the same time ensuring that $[\text{Re}(\text{CN-}t\text{-Bu})_4(\text{PPh}_3)_2]^+$ was not oxidized ($E_{1/2} = +0.81$ V vs SCE).¹² By monitoring this reaction by CV we were able to show that rapid conversion to $[\text{Re}(\text{CN-}t\text{-Bu})_4(\text{PPh}_3)_2]^+$ occurred and that no significant quantities of $[\text{Re}_2(\mu\text{-H})_3\text{H}_2(\text{PPh}_3)_4(\text{CN-}t\text{-Bu})_2]^{n+}$ remained.

Acknowledgment. Support from the National Science Foundation (Grant No. CHE82-06117) is gratefully acknowledged. The Varian XL-200 spectrometer was purchased with funds from the National Science Foundation (Grant No. CHE80-04246 to Purdue).

Registry No. $\text{Re}_2\text{H}_8(\text{PPh}_3)_4$, 66984-37-0; $\text{Re}_2\text{H}_8(\text{PETPh}_2)_4$, 66984-38-1; $\text{Re}_2\text{H}_8(\text{PEtPh}_2)_4$, 63313-85-9; $\text{Re}_2\text{H}_8(\text{AsPh}_3)_4$, 87901-15-3; $[\text{Re}_2\text{H}_8(\text{PPh}_3)_4]\text{PF}_6$, 86664-86-0; $[\text{Re}_2\text{H}_8(\text{PETPh}_2)_4]^+$, 87882-98-2; $[\text{Re}_2\text{H}_8(\text{PEtPh}_2)_4]^+$, 87882-99-3; $[\text{Re}_2\text{H}_8(\text{AsPh}_3)_4]^+$, 87883-00-9; $[\text{Re}_2\text{H}_7(\text{PPh}_3)_4(\text{NCMe})]\text{PF}_6$, 86664-85-9; $[\text{Re}_2\text{H}_7(\text{PPh}_3)_4(\text{NCtEt})]\text{PF}_6$, 87883-02-1; $[\text{Re}_2\text{H}_7(\text{PPh}_3)_4(\text{NCPh})]\text{PF}_6$, 87883-04-3; $[\text{Re}_2\text{H}_7(\text{PPh}_3)_4(\text{CN-}t\text{-Bu})]\text{PF}_6$, 86664-91-7; $[\text{Re}_2\text{H}_7(\text{PPh}_3)_4(\text{NCMe})](\text{PF}_6)_2$, 86664-88-2; $[\text{Re}_2\text{H}_7(\text{PPh}_3)_4(\text{NCtEt})](\text{PF}_6)_2$, 87883-06-5; $[\text{Re}_2\text{H}_7(\text{PPh}_3)_4(\text{NCPh})](\text{PF}_6)_2$, 87883-08-6; $[\text{Re}_2\text{H}_7(\text{PPh}_3)_4(\text{CN-}t\text{-Bu})](\text{PF}_6)_2$, 86664-93-9; $[\text{Re}_2\text{H}_5(\text{PPh}_3)_4(\text{CN-}t\text{-Bu})_2]\text{PF}_6$, 86676-29-1; $[\text{Re}_2\text{H}_5(\text{PPh}_3)_4(\text{CN-}t\text{-Bu})_2](\text{PF}_6)_2$, 86676-31-5; $[\text{Re}(\text{CN-}t\text{-Bu})_4(\text{PPh}_3)_2]\text{PF}_6$, 80006-29-7; $\text{ReOCl}_3(\text{AsPh}_3)_2$, 87863-04-5; $\text{Ph}_3\text{C}^+\text{PF}_6^-$, 437-17-2; $\text{C}_7\text{H}_7^+\text{PF}_6^-$, 29630-11-3; NO^+PF_6^- , 16921-91-8.

(27) The mechanism by which the reactive dicationic species $[\text{Re}(\mu\text{-H})_3\text{H}_2(\text{PPh}_3)_4(\text{CN-}t\text{-Bu})_2](\text{PF}_6)_2$ is reduced back to its relatively unreactive monocationic congener is at present unknown.

Template Effects. 6.¹ The Effect of Alkali Metal Ions on the Formation of Benzo-3*x*-crown-*x* Ethers over a Wide Range of Ring Sizes

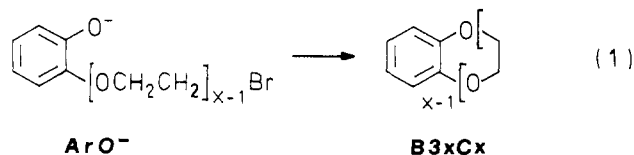
Luigi Mandolini* and Bernardo Masci*

Contribution from Centro C.N.R. di Studio sui Meccanismi di Reazione, c/o Istituto di Chimica Organica, Università "La Sapienza" di Roma, P.le Aldo Moro, 2 00185 Roma, Italy.

Received April 12, 1983

Abstract: The rate of formation of benzo-3*x*-crown-*x* ethers with $x = 4, 5, 7, 10,$ and 16 via intramolecular alkylation of $\alpha\text{-OC}_6\text{H}_4(\text{OCH}_2\text{CH}_2)_{x-1}\text{Br}$ in 99% aqueous Me_2SO was found to be markedly affected by added alkali metal bromides. Catalysis or inhibition was observed, depending on the cation-substrate pair. Combination of the present results with those previously reported for the formation of B18C6 offers a large variety of patterns. The magnitude of the observed effects ranges over four powers of ten. The dependence of the observed rates (k_{obsd}) on metal ion concentration was expressed in terms of independent contributions from free and cation-paired aryl oxide ions, whose relative weights are ruled by the rate constants k_f and k_{ip} , respectively, and by the ion-pairing association constants K_{ArO^-} . A self-consistent analysis was used to derive numerical values of the above parameters. A definite contribution from an additional reaction path involving two metal ions was detected in the case of the K^+ -catalyzed formation of B30C10. The equilibrium constants K_C for associations between many cation-crown pairs were also determined under the same conditions. A comparative analysis of structure and metal ion effects on the extent of interaction of the alkali metal ions with the reactants, transition states, and reaction products shows that the cation interaction in the transition state is strongly reminiscent of the host-guest interactions found in the cation-B3*x*C*x* complexes. The catalytic efficiency of the alkali metal ions ($\log k_{\text{ip}}/k_f$) shows a definite tendency to parallel the strength of interaction with the reaction products ($\log K_C$), thus indicating that a metal ion capable of binding strongly with a crown ether is also a good catalyst for the formation of the crown ether itself.

In a recent paper² on the formation of benzo-18-crown-6 in 99% aqueous Me_2SO (eq 1, $x = 6$), we found that the catalytic effi-

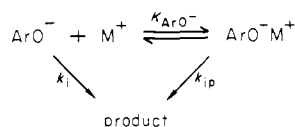


ciency of the alkali metal ions was closely related to the strength of interaction between the alkali metal ions and the reaction product, B18C6. Since associations between alkali metal ions and crown ethers are known to be highly dependent upon both the

(1) Part 5: Ercolani, G.; Mandolini, L.; Masci, B. *J. Am. Chem. Soc.*, **1983**, *105*, 6146.

(2) Illuminati, G.; Mandolini, L.; Masci, B. *J. Am. Chem. Soc.* **1983**, *105*, 555.

Scheme I



nature of the metal ion and the ring size of the crown ether,³ changes in the chain length of the phenoxide reactant ArO⁻ are expected to produce highly structured reactivity patterns exhibiting features other than those observed in the formation of benzo-18-crown-6.

In this paper we report on a detailed kinetic investigation of the template effect of alkali metal ions on the formation of B3xCx ethers with ring sizes of 12, 15, 21, 30, and 48 atoms ($x = 4, 5, 7, 10,$ and $16,$ respectively) in 99% aqueous Me₂SO at 25.0 °C. In many cases the equilibrium constants K_C for association between the alkali metal ions and the crown ethers have been obtained under the same conditions from independent equilibrium measurements. Combined with our previous results related to the formation of B18C6,² the data from the present work provide a wide picture of metal ion and ring-size effects on the formation of crown ethers catalyzed by alkali metal ions.

Results

Rate Measurements and Treatment of Kinetic Data. The cyclization of the phenoxide reactants to the corresponding crown ethers was followed in 99% Me₂SO at 25.0 °C by monitoring the disappearance of the phenoxide absorption in the region of 300–315 nm in very dilute substrate solutions (ca. $1\text{--}2 \times 10^{-4}$ M). These solutions were prepared by neutralizing solutions of the parent phenols with a calculated amount of (CH₃)₄NOH stock solution. The alkali metal ions were added as bromides over a wide concentration range up to 0.1–0.2 M. In many cases the effect of added tetraalkylammonium bromides was also studied. The reactions followed first-order kinetics up to high conversions in all cases. A complete list of observed rate constants k_{obsd} is given in the Experimental Section. Log–log plots of k_{obsd} against added salt concentration are shown in Figure 1 for the individual crown ethers. Clearly, either rate enhancement or rate retardation results from the addition of the alkali bromides. In contrast, the effect of tetraalkylammonium salts is very small, which indicates that the k_{obsd} values obtained when the stoichiometric Me₄N⁺ ion is the sole cation present (given by the solid horizontal lines in Figure 1) are to be interpreted as the rate constants k_i for reactions of the free ArO⁻ ions. The effect of the alkali metal ions may be interpreted on the hypothesis of 1:1 associations with ArO⁻ and of independent contributions to the overall reaction from the free ion ArO⁻ and the ion pair ArO⁻M⁺ (Scheme I). From Scheme I the basic equation

$$k_{\text{obsd}} = \frac{k_i + k_{\text{ip}}K_{\text{ArO}^-}\gamma_{\pm}^2[\text{M}^+]}{1 + K_{\text{ArO}^-}\gamma_{\pm}^2[\text{M}^+]} \quad (2)$$

is derived, where K_{ArO^-} is the equilibrium constant for association. As was shown in a previous paper,² eq 2 is found to closely represent the influence of alkali metal ions on the formation of B18C6 (eq 1, $3x = 18$) and other Williamson-type reactions in 99% Me₂SO, and also may be applied to the reactions of the present work. The results are summarized in Table I. The solid lines in Figure 1 are plots which are calculated using eq 2. With the sole exception of the high concentration range of the K⁺-catalyzed formation of B30C10 (Figure 1D), eq 2 fits the data remarkably well.

For many reactions (Na⁺, K⁺, Rb⁺, and Cs⁺ in the formation of B15C5; K⁺, Rb⁺, and Cs⁺ in the formation of B21C7 and

Table I. Rate and Equilibrium Constants for the Alkali Metal Ion Assisted Crown Ether Forming Reactions 1 in 99% Me₂SO at 25.0 °C^a

		k_{ip}/k_i ^b	log K_{ArO^-} ^c	log K_{T^+}	log K_C ^c	log K_{T^+}/K_C
B12C4	Li ⁺	0.044	3.02	1.67		
	Na ⁺	(0.78)	(2.87)	(2.76)		
	K ⁺	(0.81)	(2.43)	(2.35)		
	Rb ⁺	(0.62)	(2.33)	(2.12)		
	Cs ⁺	(0.50)	(2.27)	(1.97)		
B15C5	Li ⁺	0.089	3.01	1.96	<i>d</i>	
	Na ⁺	11.5	2.87	3.93	0.98	2.95
	K ⁺	7.32	2.43	3.30	1.29	2.01
	Rb ⁺	4.64	2.33	3.00	1.23	1.77
	Cs ⁺	2.75	2.27	2.71	1.13	1.58
B18C6 ^e	Li ⁺	<0.01	3.05	<1	<i>d</i>	
	Na ⁺	6.03	2.62	3.50	1.70	1.80
	K ⁺	100	2.51	4.51	2.85	1.66
	Rb ⁺	42.7	2.41	4.04	2.49	1.55
	Cs ⁺	19.1	2.26	3.54	2.25	1.29
B21C7	Li ⁺	<0.01	3.01	<1	<i>d</i>	
	Na ⁺	0.27	2.69	2.12	<i>d</i>	
	K ⁺	8.07	2.58	3.49	1.94	1.55
	Rb ⁺	21.1	2.41	3.74	2.66	1.08
	Cs ⁺	25.5	2.30	3.71	2.53	1.18
B30C10	Li ⁺	<0.01	3.02	<1	<i>d</i>	
	Na ⁺	0.095	2.77	1.75	<i>d</i>	
	K ⁺ ^f	(1.48)	(2.58)	(2.76)	1.25	(1.51)
	Rb ⁺	3.91	2.42	3.01	1.57	1.45
	Cs ⁺	2.25	2.43	2.78	1.38	1.40
B48C16	Li ⁺	<0.01	3.08	<1		
	Na ⁺	0.082	2.72	1.64		
	K ⁺	(0.51)	(2.58)	(2.29)		
	Rb ⁺	(0.68)	(2.42)	(2.25)		
	Cs ⁺	(0.81)	(2.43)	(2.34)		

^a The log K_{ArO^-} values given in parentheses are equal to those of the closest homologues whose K_{ArO^-} are known (see text). The corresponding k_{ip}/k_i and log K_{T^+} values, also given in parentheses, rely upon these estimates. ^b Accuracy is about $\pm 10\%$. ^c Error limits are probably in the range of $\pm 0.05\text{--}0.1$. ^d No UV evidence for significant association was obtained. ^e Data from ref 2. ^f For the kinetic contribution involving two K⁺ ions, see text.

B30C10), the metal ions are rate enhancing, i.e., $k_{\text{ip}} > k_i$, and, apart from the effect of K⁺ in the formation of B30C10, the related rate profiles (Figure 1B, 1C, 1D) are sigmoid shaped with positive first derivatives. All these profiles show a pronounced tendency to approach saturation at high salt concentrations.

The effect of Li⁺ is always rate depressing, i.e., $k_{\text{ip}} < k_i$. As was found to be the case with B18C6,² for the formation of the larger crowns, namely, B21C7, B30C10, and B48C16, no contribution from the ion pair to the overall reaction could be detected, which means that the quantity $k_{\text{ip}}K_{\text{ArO}^-}\gamma_{\pm}^2[\text{M}^+]$ of eq 2 is negligible with respect to k_i even at the higher LiBr concentrations. This allows us to estimate that the reactivity of the ion pair is at least two orders of magnitude lower than that of the free anion. However, with the smaller crowns, namely, B12C4 and B15C5, significant contributions from the ion pair were detected. This is clearly shown by comparison of the related rate profiles (Figure 1A and 1B) which are sigmoid shaped and show a negative first derivative, with those recorded in Figure 1C–E, where log k_{obsd} drops steeply and monotonically on increasing log [Li⁺]. Similar negative sigmoid-shaped profiles are shown by Na⁺ with the larger crown ethers, namely, B21C7 (Figure 1C), B30C10 (Figure 1D), and B48C16 (Figure 1E).

There are a number of cases where the rate-retarding influence of the cation is very small. These are the formation of B12C4 in the presence of Na⁺, K⁺, Rb⁺, and Cs⁺, and the formation of B48C16 with K⁺, Rb⁺, and Cs⁺ present. In these cases the magnitude of the observed effect is not large enough to permit either the recognition of negative sigmoids in the related rate profiles or meaningful application of an equation with two adjustable parameters, such as eq 2. We nevertheless assume that these cases also obey eq 2 and take as a reasonable estimate for

(3) (a) Lamb, J. D.; Izatt, R. M.; Christensen, J. J.; Eatough, D. J. In "Coordination Chemistry of Macrocyclic Compounds"; Melson, G. A., Ed.; Plenum Press: New York, 1979. (b) Lamb, J. D.; Izatt, R. M.; Christensen, J. J. In "Progress in Macrocyclic Chemistry"; Izatt, R. M., Christensen, J. J., Eds.; Wiley: New York, 1981; Vol. 2. (c) Poonla, N. S.; Bajaj, A. V. *Chem. Rev.* **1979**, *79*, 389.

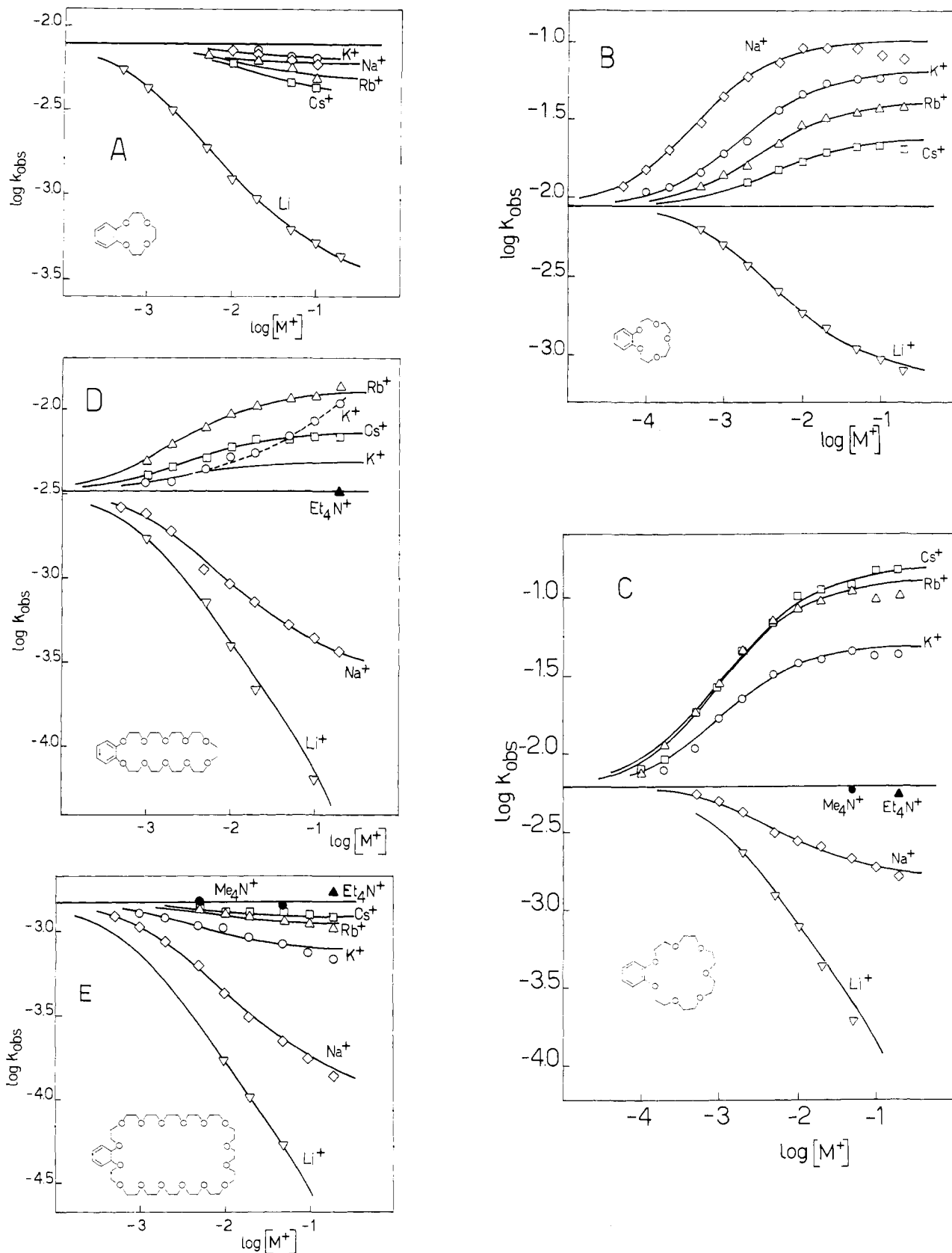


Figure 1. Effect of tetraalkylammonium and alkali metal bromides on the rate of the crown ether forming reactions 1 in 99% Me₂SO at 25.0 °C: (A) B12C4, (B) B15C5, (C) B21C7, (D) B30C10, (E) B48C16. The horizontal lines represent the rate coefficients in the absence of added salts. The points are experimental (k_{obs} in s⁻¹) and the full lines are calculated using eq 2. The dashed line in D is calculated using eq 3.

the unknown K_{ArO^-} values the corresponding values for the closest homologues whose K_{ArO^-} 's are known. The validity of this estimation procedure is corroborated by the substantial insensitivity of K_{ArO^-} to the length of the polyether side chain (Figure 2). When the estimated K_{ArO^-} values are introduced into eq 2, the

latter becomes an equation with only one unknown parameter, i.e., k_{ip} , which may be determined from the slope of plots (not shown here) of $k_{\text{obs}}(1 + K_{\text{ArO}^-}\gamma_{\pm}^2[\text{M}^+])$ vs. $K_{\text{ArO}^-}\gamma_{\pm}^2[\text{M}^+]$.

We now turn to the K⁺-catalyzed formation of B30C10. At first the profile runs parallel to that of Cs⁺, but at concentrations

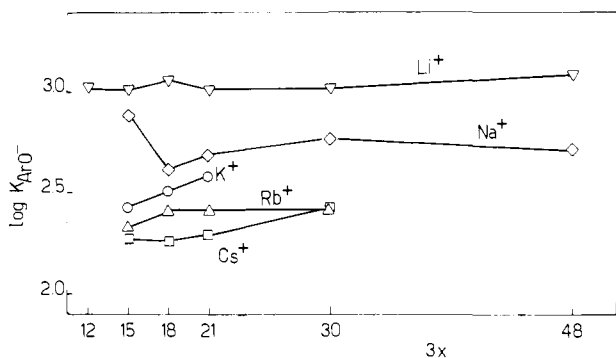
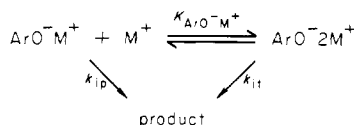


Figure 2. Effect of the length of the polyether side chain on the ion-pairing tendency of ArO^- with alkali metal ions in 99% Me_2SO at 25.0 $^\circ\text{C}$.

Scheme II



greater than 0.02 M the shape is markedly different. We interpret this behavior as due to the superposition of an additional reaction path which passes through a transition state ($\text{T}^*\text{2M}^+$) that requires the intervention of two M^+ ions, as is shown in Scheme II, where $K_{\text{ArO}^-\text{M}^+}$ is the equilibrium constant for association of M^+ to ArO^-M^+ to give the triple ion $\text{ArO}^-\text{2M}^+$. Combination of Scheme II with Scheme I leads to 3.

$$k_{\text{obsd}} = \frac{k_i + k_{\text{ip}}K_{\text{ArO}^-\gamma_{\pm}^2}[\text{M}^+] + k_{\text{it}}K_{\text{ArO}^-\text{M}^+\gamma_{\pm}^2}[\text{M}^+]^2}{1 + K_{\text{ArO}^-\gamma_{\pm}^2}[\text{M}^+] + K_{\text{ArO}^-\text{M}^+\gamma_{\pm}^2}[\text{M}^+] + K_{\text{ArO}^-\text{M}^+\gamma_{\pm}^2}[\text{M}^+]^2} \quad (3)$$

There are four unknown parameters in eq 3, namely, k_{ip} , K_{ArO^-} , k_{it} , and $K_{\text{ArO}^-\text{M}^+}$. However, a few simplifications are possible. First, K_{ArO^-} can be assumed to be equal to 384 M^{-1} , i.e., to the value of the closest lower homologue. Second, k_{ip} can be estimated as described above from the data at low concentrations ($[\text{M}^+] \leq 0.02 \text{ M}$) where the $[\text{M}^+]^2$ terms are relatively unimportant and eq 3 reduces to eq 2. The result is a k_{ip} value of $4.85 \times 10^{-3} \text{ s}^{-1}$. Upon introduction of the known k_{ip} and K_{ArO^-} values, eq 3 becomes a two-parameter equation which can be conveniently rearranged into linear form (eq 4). The unknown parameters k_{it} and $K_{\text{ArO}^-\text{M}^+}$

$$k_{\text{obsd}} = k_{\text{it}} - \frac{1}{K_{\text{ArO}^-\text{M}^+}} \left[\frac{k_{\text{obsd}} + K_{\text{ArO}^-\gamma_{\pm}^2}[\text{M}^+](k_{\text{obsd}} - k_{\text{ip}}) - k_i}{K_{\text{ArO}^-\gamma_{\pm}^2}[\text{M}^+]^2} \right] \quad (4)$$

were estimated from the intercept and slope, respectively, of a plot of k_{obsd} against the quantity which is given in square brackets in eq 4. The linearity of this plot (not shown here) is good for points at high concentration, but points at low concentration where either $(k_{\text{obsd}} - k_i)$ or $(k_{\text{obsd}} - k_{\text{ip}})$ is a small quantity, show significant scatter. The results are $k_{\text{it}} = 1.8 \times 10^{-2} \text{ s}^{-1}$ and $K_{\text{ArO}^-\text{M}^+} = 4.3 \text{ M}^{-1}$. When all the estimated parameters are introduced into eq 4, the calculated rate profile is that given by the dashed line of Figure 1D, which is seen to fit the data over the entire concentration range.

It is noteworthy that at $[\text{Rb}^+] = 0.2 \text{ M}$ the specific rate k_{obsd} of the Rb^+ -catalyzed cyclization to form B30C10 (Figure 1D) is somewhat larger than that calculated using eq 2. Although the difference is small, it does not seem to be due to experimental errors, as shown by repeated experiments. It could be attributed to the appearance of an $[\text{M}^+]^2$ contribution also in the Rb^+ case.

Equilibrium Measurements. $\text{M}^+\cdot\text{B3xCx}$ Complexes, $x = 5, 7,$ and 10 . The determination of the equilibrium constants for 1:1 association of the crown ethers with the alkali metal ions in 99% Me_2SO at 25 $^\circ\text{C}$ was carried out as before² on the basis of changes

in the UV spectra of the crown ethers arising from additions of increasing amounts of the alkali bromides. In a number of cases no UV evidence for significant association was obtained which is indicative of K_{C} values smaller than 10 M^{-1} . The results are listed in Table I.

Discussion

The metal template cyclization studies which are described in the present work provide clean-cut examples of rate acceleration or retardation by alkali metal ions which correctly fit into a kinetic model that involves independent contributions from free and cation-paired phenoxide ions. A self-consistent analysis of the kinetic data permits a dissection of contributions from the two parallel reaction paths and affords rate constants for the reactions of the free ions (k_i) and of the ion pair (k_{ip}), together with the ion-pairing equilibrium constant (K_{ArO^-}). In one case (B30C10, K^+) a definite contribution from a third reaction path was detected, namely, one where two M^+ ions are involved in the transition state.

In addition to the equilibrium constants which are derived from the kinetics, independent measurements have provided association constants (K_{C}) for many M^+ -crown ether pairs.

Before discussing the effects of structure on reactivity, we shall examine structural effects on the stabilities of the ion pairs ArO^-M^+ and of the $\text{M}^+\cdot\text{B3xCx}$ complexes.

The set of K_{ArO^-} values given in Table I and plotted in Figure 2 exhibits an insensitivity to the length of the polyether chain and a gradual decrease in stability order in going from Li^+ to Cs^+ . This confirms our previous analysis² which was based on the ion-pairing behavior of ArO^- (with $x = 6$) vs. a series of phenoxide ions including the unsubstituted phenoxide and the 2-methoxyphenoxide ions. The main features can be summarized as follows: (i) as a result of contact pairing in the ArO^-M^+ pairs, coulombic interaction provides a major driving force for association and is responsible for the inverse relationship of stabilities to cation size; (ii) chelate interaction with the oxygen atom connecting the side chain to the aromatic ring is important for all the metal ions; and (iii) additional stabilization from coordination with the remaining oxygen donors of the polyether chain is significant in the case of the heavier metal ions, still appreciable with Na^+ , but absent with Li^+ . The $\log K_{\text{ArO}^-}$ values for the heavier metal ions show a tendency to increase on increasing chain length, but the magnitude of the enhancements is not much greater than the experimental uncertainties. In addition to the remarkable constancy of the $\log K_{\text{ArO}^-}$ values for Li^+ for which multiple coordination is unimportant, a stability constant drop by some 0.2 log unit in going from $x = 5$ to 6 in the case of Na^+ is noteworthy. However, it is difficult to say whether the effect is real or not.

In marked contrast to the substantial insensitivity of the K_{ArO^-} values to the length of the polyether chain is the highly structured pattern which is displayed by the K_{C} values (Figure 3). This pattern is in agreement with the well-known concept of the fit between the cation and ligand cavity sizes.³ There is a pronounced tendency for the higher crown ethers to give the stronger associations with the larger metal ions. However, B15C5 shows poor cation selectivity in agreement with similar results reported by Izatt et al.⁴ for the association of 15C5 with alkali metal ions in methanol. Noting that even Na^+ is too large to enter the cavity of the 15-membered macrocycle, as was suggested by molecular models and by crystallographic data for the $\text{Na}^+\cdot\text{B15C5}$ complex,⁵ Izatt et al.⁴ pointed out that for cations which are too large to enter into the ligand cavity, selectivity is not determined by the size correlation. We note, however, that whereas the $K_{\text{C}}^{\text{Na}^+}/K_{\text{C}}^{\text{K}^+}$ ratio for B15C5 is 0.5 and 1.0 in the good cation-solvating media of Me_2SO and MeOH ,⁶ respectively, a value as high as 14 is observed in the poorer cation-solvating medium of MeCN ,⁷ which indicates that cation solvation may also play a major role in

(4) Lamb, J. D.; Izatt, R. M.; Swain, C. S.; Christensen, J. J. *J. Am. Chem. Soc.* **1980**, *102*, 475.

(5) Bush, M. A.; Truter, M. R. *J. Chem. Soc., Perkin Trans. 2* **1972**, 341.

(6) Unpublished results from this laboratory.

(7) Hofmanova, A.; Koryta, J.; Brezina, M.; Mittal, L. *Inorg. Chim. Acta* **1978**, *28*, 73.

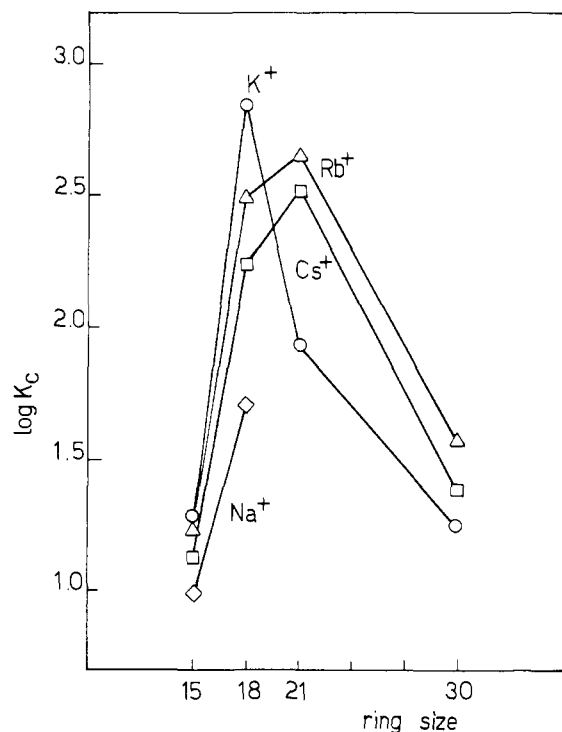


Figure 3. Ring size effect for the association of alkali metal ions with benzo crown ethers in 99% Me₂SO at 25.0 °C.

determining selectivity.⁸ In our opinion, these data suggest that B15C5 is an inherently better ligand for Na⁺ than for K⁺ because of the greater size correspondence of the former, but that this tendency is counteracted by a good cation-solvating medium, which interacts more strongly with the smaller cation. In other words, interaction between Na⁺ and B15C5 in MeCN, if not necessarily one where Na⁺ is completely buried in the host cavity, is at least one where Na⁺ is partly accommodated within the host cavity. This gives rise to a tight interaction which requires extensive cation desolvation. However, in good cation-solvating solvents like Me₂SO and MeOH where desolvation of M⁺ is more energy demanding,⁹ the M⁺-B15C5 complexes are probably more loosely bound so that any advantage of Na⁺ over K⁺ disappears.

Let us now consider the chain length and metal ion effects on the rate of the templated crown ether forming cyclizations. It is of interest to compare the k_{ip}/k_i values from Table I with those for the reaction of *o*-OC₆H₄(OCH₂CH₂)₄OCH₃ with BuBr. For this reaction we found² that the k_{ip}/k_i ratio was 0.069 for Cs⁺, 0.071 for Rb⁺, 0.065 for K⁺, 0.035 for Na⁺, and too small to measure in the case of the Li⁺ reaction for which an upper limit of 0.01 was set. When these data are compared with those in Table I, it is noted that in most cases the alkali metal ions exert a larger inhibitory effect on the intermolecular reaction than on the intramolecular ones. We assume that the given intermolecular reaction provides a reasonable estimate for the inherent nucleophilicity decrease of the aryl oxide nucleophile upon cation pairing. Therefore, a template effect is operating not only in cyclizations where catalysis occurs, but also in those cases in which there is rate inhibition upon cation pairing, apart from cyclizations leading to B18C6 and to the larger crown ethers as carried out in the presence of Li⁺, where k_{ip} was too small to measure.

The log (k_{ip}/k_i) values from Table I are plotted vs. ring size in Figure 4. Comparison with Figure 2 and 3 clearly shows that the structural effect on rates exhibits a pattern which resembles that found for association of metal ions with the crown ether products, but not that with the aryl oxide reactants. This observation reinforces the conclusion that catalysis is strictly related

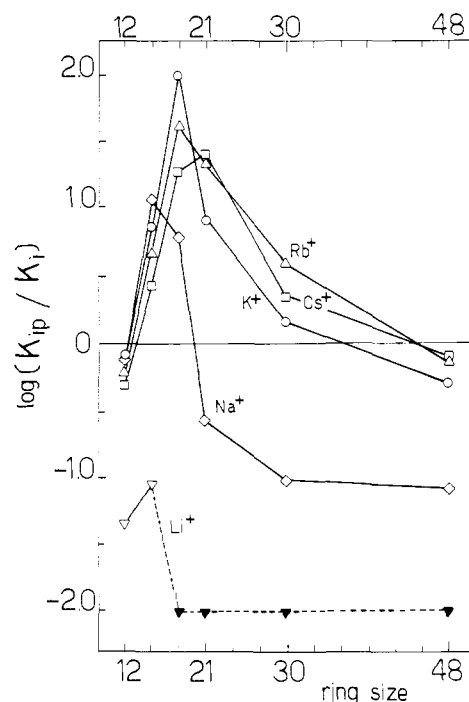


Figure 4. Catalysis and inhibition by alkali metal ions on the crown ether forming reactions 1 in 99% Me₂SO at 25.0 °C. Plot of log (k_{ip}/k_i) vs. size of the crown ether to be formed. The full triangles represent upper reactivity limits.

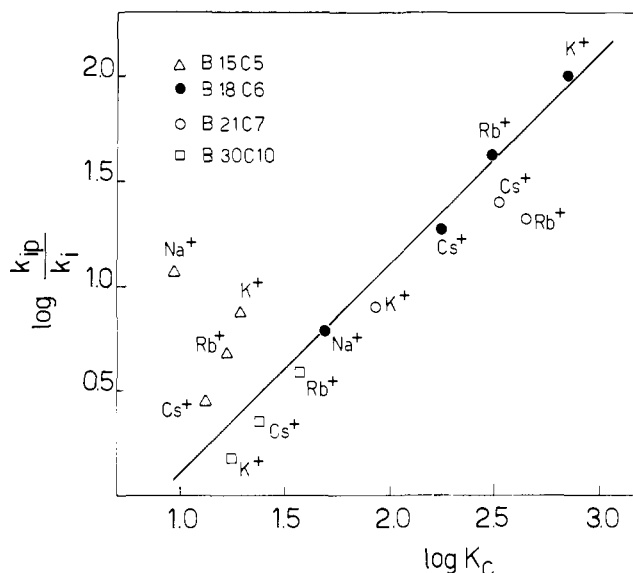


Figure 5. Catalytic efficiency of the alkali metal ions on the crown ether forming reactions 1 vs. association with the crown ether products. The slope of the straight line is 1.00 and the intercept is -0.90.

to those factors which govern the strength of association with the reaction product and is consistent with the general conclusion which has been drawn from synthetic experiments¹⁰ in that there is a relation between the template effect and the correspondence between the cation diameter and ligand cavity size.

In the case of the M⁺-catalyzed formation of B18C6 we found² that to a good approximation log (k_{ip}/k_i) was linearly related to log K_c through the relationship

$$\log k_{ip}/k_i = \log K_c - 0.90 \quad (5)$$

where the constant -0.90 reflects the loss of nucleophilicity of ArO⁻

(8) (a) Holland, H.; Ringseth, J. A.; Brun, T. S. *J. Solution Chem.* **1979**, *8*, 779. (b) Michaux, G.; Reisse, J. *J. Am. Chem. Soc.* **1982**, *104*, 6895.
 (9) Burgess, J. "Metal Ions in Solution"; Ellis Horwood: Chichester, U. K., 1978; Chapter 7.

(10) (a) Reinhoudt, D. N.; Gray, R. T.; Smit, C. J.; Veenstra, I. *Tetrahedron* **1976**, *32*, 1161. (b) Cook, F. L.; Caruso, T. C.; Byrne, M. P.; Bowers, C. W.; Speck, C. L.; Liotta, C. L. *Tetrahedron Lett.* **1974**, 4029.

upon cation pairing. A plot of $\log(k_{ip}/k_i)$ vs. $\log K_C$ which is extended to cover all M^+ and crown ether pairs for which data are available is presented in Figure 5. Although it is not a perfectly linear relationship, this plot shows an unmistakable trend. Thus a metal ion which is capable of associating strongly with a crown ether is a good catalyst for the formation of that crown ether, and cation selectivity in equilibria is roughly parallel to cation selectivity in rates. This conclusion is also confirmed on a qualitative basis by the observation that whenever a metal ion exerts a rate-retarding effect (Table I), the corresponding K_C value is too small to measure.

For the plot in Figure 5, if the markedly deviant point for Na^+ , B15C5 is neglected, the standard deviation of points from the indicated line is 0.24 log unit with no deviation being larger than twice the standard deviation. This is remarkable, since linear free energy relationships often fail when the structural changes occur close to the reaction zone.¹¹

In order to discuss properly the question of the adherence of the data to, or the deviations from, the straight line, it is useful to summarize briefly the theoretical interpretation which has been presented² in support of eq 5. According to transition state theory, the quantity K_{T^*} which is calculated as

$$K_{T^*} = (k_{ip}/k_i)K_{ArO^-} \quad (6)$$

has the meaning of the equilibrium constant for the conversion of the transition state (T^*) which does not contain M^+ to one (T^*M^+) which does contain M^+ .¹² A comparison of metal ion effects on K_{ArO^-} , K_{T^*} , and K_C for the B18C6 case strongly suggested a host-guest type interaction in T^*M^+ .^{1,2} A simple model was developed,^{1,2} according to which the geometry of the cation-paired transition states T^*M^+ was well mimicked by that of the $M^+ \cdot B18C6$ complexes, and the extra stability of the former with respect to the latter was solely due to coulombic interaction of M^+ with the negative charge of T^* .

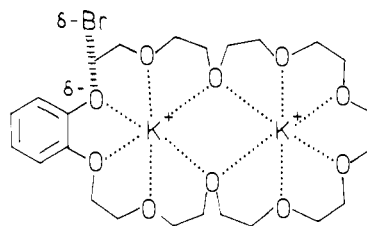
Let us now turn to consider the formation of the crown ethers other than B18C6 (Table I). Again we find that in all cases the cation interaction in the transition state is stronger than in the reaction product (i.e., $K_{T^*} > K_C$). However, the K_{T^*}/K_C ratios for each metal ion are not strictly independent of the size of the crown ether as would be required by the simple model outlined above. Were the K_{T^*}/K_C ratios for each metal ion independent of ring size, all the points in the plot of Figure 5 would lie very close to a line of slope 1 and intercept -0.90 . Deviations of the K_{T^*}/K_C ratios are not, however, very serious, except in the case of the Na^+ -catalyzed formation of B15C5. We conclude, therefore, that in general the templated crown ether forming cyclizations do not deviate very seriously from a simple model which assigns to the M^+ -paired transition states the geometries of the corresponding M^+ -crown ether complexes.

The markedly deviant behavior in the Na^+ , B15C5 case suggests that the structure of the $Na^+ \cdot B15C5$ complex is no longer a suitable model for the Na^+ -paired transition state. This phenomenon is possibly related to the looseness of the $Na^+ \cdot B15C5$ complex which was previously discussed. Accordingly, we suggest that coulombic interaction between the negative charge in the transition state and the metal ion can render the structure of T^*M^+ tighter than that of the corresponding M^+ -crown ether complex. This enforced proximity between the polyether chain and the cation should provide an additional stabilizing interaction through enhanced multiple coordination. One should find this kind of effect to be significant with the smaller cations, for which coulombic interactions are stronger, and with the smaller rings, whose cavities are not large enough as to accommodate the cations and remove completely their solvation shells. Indeed, we find that the 15-membered transition state binds cations with an efficiency which decreases regularly in going from Na^+ to Cs^+ , even though poor selectivity is observed in the $M^+ \cdot B15C5$ complexes (Table I). This agrees with the observation that in the case of B15C5 the alkali

metal ions show deviations from the straight line in Figure 5 which decrease in the order $Na^+ > K^+ > Rb^+ > Cs^+$. Also consistent with this hypothesis is the observation that the K_{T^*} values for B12C4 formation follow the same order as do the K_{T^*} values for the formation of B15C5, even though a direct comparison of the former with the stabilities of the $M^+ \cdot B12C4$ complexes is not possible because of the unavailability of the K_C values for B12C4.

For the Li^+ -paired 12- and 15-membered transition states, the lack of the corresponding K_C values prevents the correlation with the linear free-energy relationship from being tested. However, on a qualitative basis, the fact that these transition states display appreciable stability, whereas those for the higher homologues do not, can be safely attributed to a host-guest interaction in accordance with the better size correspondence of Li^+ to the smaller rings.

The apparent ability of the transition state, which leads to B30C10, to bind two K^+ ions cannot be correlated with the association constant for B30C10 with two K^+ which has not been determined. However, 1:2 complexes between large crown ethers and alkali cations are known to occur in solution¹³ and have been isolated in the solid state.¹⁴ X-ray crystallographic studies^{14b,c} indicate that the structure of these complexes is of the host-guest type, which renders it likely that also in the transition state $T^* \cdot 2K^+$ leading to B30C10 the two K^+ ions are embedded in the ligand cavity as depicted.



Experimental Section

Most techniques and apparatus have been previously reported,² as was the preparation of the parent phenols of compounds ArO^- and that of B30C10.¹⁵ B15C5 was prepared as described by Pedersen.¹⁶ B21C7 was prepared under conditions similar to those used for the kinetic runs: 1.5 mL of 1.1 M Me_4NOH was added at room temperature to a stirred solution of 700 mg (1.60 mmol) of *o*-hydroxyphenyl 3,6,9,12,15-pentaoxa-17-bromoheptadecyl ether and 0.6 g (5 mmol) of KBr in 50 mL of Me_2SO . After 1 h water was added and the product was continuously extracted with hexane and purified by elution from a silica gel column with $EtOAc/MeOH$ (75:1). The colorless oil obtained therefrom (1.47 mmol, 92% yield) was further purified by microdistillation *in vacuo*. The 1H NMR spectrum was as expected; $M^+ m/e$ 356.

Reference is made to the previous paper² for comments on the rate and equilibrium measurements, for elaboration of the data, and the evaluation of the activity coefficients.

Rate constants k_{obsd} are reported in the following listing, for the various alkali and tetraalkylammonium bromide concentrations in molar units, which are given in parentheses. The correlation coefficients r for the treatment according to eq 7 in ref 2 are also reported:

Reaction 1, $x = 4$; $k_i = 7.79 \times 10^{-3} s^{-1}$. Li^+ : 5.40×10^{-3} (5×10^{-4}), 4.26×10^{-3} (1×10^{-3}), 3.14×10^{-3} (2×10^{-3}), 1.88×10^{-3} (5×10^{-3}), 1.24×10^{-3} (1×10^{-2}), 9.46×10^{-4} (2×10^{-2}), 6.25×10^{-4} (5×10^{-2}), 5.21×10^{-4} (0.1), 4.30×10^{-4} (0.2); $r = 0.9998$.

Na^+ : 7.16×10^{-3} (1×10^{-2}), 6.81×10^{-3} (2×10^{-2}), 6.46×10^{-3} (5×10^{-2}), 5.87×10^{-3} (0.1).

K^+ : 7.06×10^{-3} (2×10^{-2}), 6.52×10^{-3} (5×10^{-2}), 6.51×10^{-3} (0.1).

Rb^+ : 6.64×10^{-3} (5×10^{-3}), 6.20×10^{-3} (2×10^{-2}), 5.73×10^{-3} (5×10^{-2}), 4.83×10^{-3} (0.1).

Cs^+ : 6.00×10^{-3} (1×10^{-2}), 4.63×10^{-3} (5×10^{-2}), 4.32×10^{-3} (0.1).

Reaction 1, $x = 5$; $k_i = 8.88 \times 10^{-3} s^{-1}$. Li^+ : 6.33×10^{-3} (5×10^{-4}), 5.15×10^{-3} (1×10^{-3}), 3.83×10^{-3} (2×10^{-3}), 2.64×10^{-3} (5×10^{-3}), 1.88×10^{-3} (1×10^{-2}), 1.49×10^{-3} (2×10^{-2}), 1.09×10^{-3} (5×10^{-2}), 9.32×10^{-4} (0.1), 7.90×10^{-4} (0.2); $r = 0.9992$.

(13) Shamsipur, M.; Popov, A. I. *J. Am. Chem. Soc.* **1979**, *101*, 4051.

(14) (a) Poonia, N. S.; Truter, M. R. *J. Chem. Soc., Dalton Trans.* **1973**, 2062. (b) Poonia, N. S.; Truter, M. R. *Ibid.* **1973**, 2469. (c) Hughes, D. L. *Ibid.* **1975**, 2374.

(15) Illuminati, G.; Mandolini, L.; Masci, B. *J. Am. Chem. Soc.* **1981**, *103*, 4142.

(16) Pedersen, C. J. *J. Am. Chem. Soc.* **1967**, *89*, 7017.

(11) Hammett, L. P. "Physical Organic Chemistry", 2nd ed.; McGraw-Hill: New York, 1970; Chapter 11.

(12) Reference 11, Chapter 5.

Na⁺: 1.17×10^{-2} (5×10^{-5}), 1.52×10^{-2} (1×10^{-4}), 2.05×10^{-2} (2×10^{-4}), 3.04×10^{-2} (5×10^{-4}), 4.49×10^{-2} (1×10^{-3}), 6.00×10^{-2} (2×10^{-3}), 7.38×10^{-2} (5×10^{-3}), 9.27×10^{-2} (1×10^{-2}), 8.97×10^{-2} (2×10^{-2}), 8.81×10^{-2} (5×10^{-2}), 8.13×10^{-2} (0.1), 7.78×10^{-2} (0.2); $r = 0.9882$.

K⁺: 1.11×10^{-2} (1×10^{-4}), 1.19×10^{-2} (2×10^{-4}), 1.45×10^{-2} (5×10^{-4}), 1.92×10^{-2} (1×10^{-3}), 2.31×10^{-2} (2×10^{-3}), 3.67×10^{-2} (5×10^{-3}), 4.68×10^{-2} (1×10^{-2}), 5.39×10^{-2} (2×10^{-2}), 5.77×10^{-2} (5×10^{-2}), 5.76×10^{-2} (0.1), 5.72×10^{-2} (0.2); $r = 0.9611$.

Rb⁺: 1.18×10^{-2} (5×10^{-4}), 1.39×10^{-2} (1×10^{-3}), 1.56×10^{-2} (2×10^{-3}), 2.25×10^{-2} (5×10^{-3}), 2.96×10^{-2} (1×10^{-2}), 3.30×10^{-2} (2×10^{-2}), 3.49×10^{-2} (5×10^{-2}), 3.72×10^{-2} (0.1), 3.74×10^{-2} (0.2); $r = 0.9485$.

Cs⁺: 1.27×10^{-2} (2×10^{-3}), 1.52×10^{-2} (5×10^{-3}), 1.70×10^{-2} (1×10^{-2}), 1.95×10^{-2} (2×10^{-2}), 2.15×10^{-2} (5×10^{-2}), 2.17×10^{-2} (0.1), 2.06×10^{-2} (0.2); $r = 0.9902$.

Reaction 1, x = 7; k_i = 6.15×10^{-3} s⁻¹. Li⁺: 2.30×10^{-3} (2×10^{-3}), 1.24×10^{-3} (5×10^{-3}), 7.77×10^{-4} (1×10^{-2}), 4.34×10^{-4} (2×10^{-2}), 1.92×10^{-4} (5×10^{-2}); $r = 0.9997$.

Na⁺: 5.56×10^{-3} (5×10^{-4}), 5.04×10^{-3} (1×10^{-3}), 4.24×10^{-3} (2×10^{-3}), 3.11×10^{-3} (5×10^{-3}), 2.77×10^{-3} (1×10^{-2}), 2.52×10^{-3} (2×10^{-2}), 2.13×10^{-3} (5×10^{-2}), 1.85×10^{-3} (0.1), 1.62×10^{-3} (0.2); $r = 0.9816$.

K⁺: 7.78×10^{-3} (2×10^{-4}), 1.08×10^{-2} (5×10^{-4}), 1.69×10^{-2} (1×10^{-3}), 2.24×10^{-2} (2×10^{-3}), 3.20×10^{-2} (5×10^{-3}), 3.81×10^{-2} (1×10^{-2}), 4.00×10^{-2} (2×10^{-2}), 4.55×10^{-2} (5×10^{-2}), 4.20×10^{-2} (0.1), 4.28×10^{-2} (0.2); $r = 0.9939$.

Rb⁺: 7.31×10^{-3} (1×10^{-4}), 1.14×10^{-2} (2×10^{-4}), 1.84×10^{-2} (5×10^{-4}), 2.83×10^{-2} (1×10^{-3}), 4.57×10^{-2} (2×10^{-3}), 7.06×10^{-2} (5×10^{-3}), 8.53×10^{-2} (1×10^{-2}), 9.40×10^{-2} (2×10^{-2}), 0.109 (5×10^{-2}), 9.66×10^{-2} (0.1), 0.101 (0.2); $r = 0.9796$.

Cs⁺: 8.01×10^{-3} (1×10^{-4}), 9.31×10^{-3} (2×10^{-4}), 1.84×10^{-2} (5×10^{-4}), 2.64×10^{-2} (1×10^{-3}), 4.38×10^{-2} (2×10^{-3}), 6.77×10^{-2} (5×10^{-3}), 0.101 (1×10^{-2}), 0.112 (2×10^{-2}), 0.122 (5×10^{-2}), 0.150 (0.1), 0.150 (0.2); $r = 0.9719$.

Me₄N⁺: 5.81×10^{-3} (5×10^{-2}).

Et₄N⁺: 5.44×10^{-3} (0.2).

Reaction 1, x = 10; k_i = 3.27×10^{-3} s⁻¹. Li⁺: 1.71×10^{-3} (1×10^{-3}), 7.22×10^{-4} (5×10^{-3}), 3.92×10^{-4} (1×10^{-2}), 2.14×10^{-4} (2×10^{-2}), 6.32×10^{-5} (0.1); $r = 0.9984$.

Na⁺: 2.58×10^{-3} (5×10^{-4}), 2.37×10^{-3} (1×10^{-3}), 1.88×10^{-3} (2×10^{-3}), 1.13×10^{-3} (5×10^{-3}), 9.27×10^{-4} (1×10^{-2}), 7.25×10^{-4} (2×10^{-2}), 5.27×10^{-4} (5×10^{-2}), 4.38×10^{-4} (0.1), 3.69×10^{-4} (0.2); $r = 0.9857$.

K⁺: 3.60×10^{-3} (1×10^{-3}), 3.69×10^{-3} (2×10^{-3}), 4.44×10^{-3} (5×10^{-3}), 5.14×10^{-3} (1×10^{-2}), 5.50×10^{-3} (2×10^{-2}), 6.83×10^{-3} (5×10^{-2}), 8.60×10^{-3} (0.1), 1.08×10^{-2} (0.2).

Rb⁺: 4.85×10^{-3} (1×10^{-3}), 6.15×10^{-3} (2×10^{-3}), 7.79×10^{-3} (5×10^{-3}), 9.38×10^{-3} (1×10^{-2}), 1.06×10^{-2} (2×10^{-2}), 1.15×10^{-2} (5×10^{-2}), 1.19×10^{-2} (0.1), 1.37×10^{-2} (0.2); $r = 0.9961$.

Cs⁺: 3.95×10^{-3} (1×10^{-3}), 4.52×10^{-3} (2×10^{-3}), 5.07×10^{-3} (5×10^{-3}), 5.98×10^{-3} (1×10^{-2}), 6.59×10^{-3} (2×10^{-2}), 6.63×10^{-3} (5×10^{-2}), 6.90×10^{-3} (0.1), 6.83×10^{-3} (0.2); $r = 0.9468$.

Et₄N⁺: 3.29×10^{-3} (0.2).

Reaction 1, x = 16; k_i = 1.48×10^{-3} s⁻¹. Li⁺: 1.70×10^{-4} (1×10^{-2}), 1.02×10^{-4} (2×10^{-2}), 5.26×10^{-5} (5×10^{-2}); $r = 0.99999$.

Na⁺: 1.22×10^{-3} (5×10^{-4}), 1.05×10^{-3} (1×10^{-3}), 8.58×10^{-4} (2×10^{-3}), 6.19×10^{-4} (5×10^{-3}), 4.20×10^{-4} (1×10^{-2}), 3.03×10^{-4} (2×10^{-2}), 2.17×10^{-4} (5×10^{-2}), 1.71×10^{-4} (0.1), 1.35×10^{-4} (0.2); $r = 0.9980$.

K⁺: 1.28×10^{-3} (1×10^{-3}), 1.20×10^{-3} (2×10^{-3}), 1.06×10^{-3} (5×10^{-3}), 1.04×10^{-3} (1×10^{-2}), 9.20×10^{-4} (2×10^{-2}), 8.39×10^{-4} (5×10^{-2}), 7.42×10^{-4} (0.1), 6.80×10^{-4} (0.2).

Rb⁺: 1.32×10^{-3} (5×10^{-3}), 1.26×10^{-3} (1×10^{-2}), 1.22×10^{-3} (2×10^{-2}), 1.12×10^{-3} (5×10^{-2}), 1.10×10^{-3} (0.1), 1.04×10^{-3} (0.2).

Cs⁺: 1.41×10^{-3} (5×10^{-3}), 1.27×10^{-3} (1×10^{-2}), 1.23×10^{-3} (2×10^{-2}), 1.25×10^{-3} (5×10^{-2}), 1.23×10^{-3} (0.1), 1.17×10^{-3} (0.2).

Me₄N⁺: 1.48×10^{-3} (5×10^{-3}), 1.42×10^{-3} (5×10^{-2}).

Et₄N⁺: 1.68×10^{-3} (0.2).

Acknowledgment. The authors wish to thank Professor Gabriello Illuminati for critically reading the manuscript.

Registry No. *o*-OC₆H₄(OCH₂CH₂)₃Br, 87494-76-6; *o*-OC₆H₄(OCH₂CH₂)₄Br, 87494-77-7; *o*-OC₆H₄(OCH₂CH₂)₆Br, 87494-78-8; *o*-OC₆H₄(OCH₂CH₂)₅Br, 87494-79-9; *o*-OC₆H₄(OCH₂CH₂)₅Br, 87494-80-2; B12C4, 14174-08-4; B15C5, 14098-44-3; B18C6, 14098-24-9; B21C7, 67950-78-1; B30C10, 77963-50-9; B48C16, 87494-81-3; Li⁺, 17341-24-1; Na⁺, 17341-25-2; K⁺, 24203-36-9; Rb⁺, 22537-38-8; Cs⁺, 18459-37-5.

Selective Syntheses Using Cyclodextrins as Catalysts. 2. Para-Oriented Carboxylation of Phenols¹

Makoto Komiyama* and Hidefumi Hirai

Contribution from the Department of Industrial Chemistry, Faculty of Engineering, University of Tokyo, Hongo, Tokyo, 113 Japan. Received May 16, 1983

Abstract: 4-Hydroxybenzoic acid and 4-hydroxy-3-methylbenzoic acid are synthesized in virtually 100% selectivities and high yields from the corresponding phenols and carbon tetrachloride by using β -cyclodextrin (β -CD) as catalyst. The selective syntheses are successfully achieved by a small molar ratio, even 0.03, of β -CD to phenols and are hardly suppressed by oxygen. Kinetic study shows that the selective catalyses by β -CD originate from both promotion of the para carboxylation and almost complete inhibition of the ortho carboxylation. Heptakis(2,6-di-*O*-methyl)- β -cyclodextrin in contrast decreases the para selectivity, showing the importance of the hydroxyl groups of β -CD in its selective catalysis. The selective catalysis by β -CD proceeds via formation of a molecular complex with the active species, probably the trichloromethyl cation. In the electrophilic attack of the active species at phenols, β -CD regulates the mutual molecular conformation between them through noncovalent interactions, resulting in highly selective para carboxylation.

Cyclodextrins (CDs), cyclic oligomers of 6-8 glucoses, have been widely used as a model of enzymes. This is mostly due to the fact that the catalyses by CDs proceed via the formation of molecular complexes of them with substrates prior to chemical

transformation. This process is identical with those of enzymatic catalyses. High substrate specificities were reported in many bond cleavage reactions such as ester hydrolyses, phosphate hydrolyses, and decarboxylation.^{2,3}

(1) Preliminary communication: M. Komiyama, H. Hirai, *Makromol. Chem., Rapid Commun.*, **2**, 661 (1981).

(2) M. L. Bender and M. Komiyama, "Cyclodextrin Chemistry", Springer-Verlag, 1978, Berlin.